

## Neutron-powder-diffraction study of nuclear and magnetic structure in $\text{YBa}_2\text{Cu}_{3-x}\text{Co}_x\text{O}_{7+y}$ with $x=0.84$ and $y=0.32$

P. Zolliker, D. E. Cox, J. M. Tranquada, and G. Shirane  
*Brookhaven National Laboratory, Upton, New York 11973-5000*  
 (Received 27 May 1988)

Neutron powder diffraction has been used to study the crystal structure and magnetic ordering of  $\text{YBa}_2\text{Cu}_{3-x}\text{Co}_x\text{O}_{7+y}$  with  $x=0.84$  and  $y=0.32$ . Rietveld refinement of the crystal structure was carried out at 295 K (space group  $P4/mmm$ ,  $a=3.888 \text{ \AA}$ ,  $c=11.636 \text{ \AA}$ ) and showed in particular that Co substitutes in the Cu(1) position of  $\text{YBa}_2\text{Cu}_3\text{O}_{7-y}$ . Long-range, three-dimensional antiferromagnetism was observed up to a Néel temperature of about 405 K. All five detected magnetic peaks could be indexed on a wave vector  $(\frac{1}{2} \frac{1}{2} \frac{1}{2})$  with  $h, k, l$  all odd, indicating a body-centered tetragonal magnetic unit cell with  $a_{\text{mag}}=a\sqrt{2}$ ,  $c_{\text{mag}}=2c$ . At 9 K the proposed magnetic structure has moments parallel to  $c$  and antiferromagnetic ordering within both Cu and Co layers. Adjacent moments in neighboring Cu layers are antiparallel whereas the small moments found in the Co layers are parallel to their adjacent moments in the neighboring Cu layers. The ordered moment was  $0.87\mu_B$  for the Cu layers and  $0.16\mu_B$  in the Co layers, respectively. With increased temperature the ordered moments in the Co layers decrease faster than those in the Cu layer. At room temperature the ordered moment was  $0.65\mu_B$  for the Cu layers with no detectable ordered moment in the Co layers.

### INTRODUCTION

In the search for an understanding of the high-temperature superconductivity found in cuprate compounds,<sup>1</sup> numerous theories have been proposed<sup>2,3</sup> emphasizing that antiferromagnetic interactions may play a key role in the understanding of the mechanism of superconductivity in this class of compounds. The observation of three-dimensional (3D), long-range antiferromagnetic order first in  $\text{La}_2\text{CuO}_{4-y}$  (Ref. 4) and later also in  $\text{YBa}_2\text{Cu}_3\text{O}_{7-y}$  (Refs. 5 and 6) with Néel temperatures of up to 500 K, provided experimental evidence for superexchange interactions in those compounds. Neutron scattering measurements on single crystals of  $\text{La}_2\text{CuO}_4$  showed evidence<sup>7</sup> for 2D correlations within  $\text{CuO}_2$  layers, even above the Néel temperature.

It is well established<sup>8</sup> that the structure of  $\text{YBa}_2\text{Cu}_3\text{O}_{7-y}$  can be viewed as a packing along the  $c$  axis of Y,  $\text{CuO}_2$ , BaO,  $\text{CuO}_{1-y}$ , BaO,  $\text{CuO}_2$  layers. The oxygen atoms in the  $\text{CuO}_{1-y}$  layers may be ordered (orthorhombic structure) or disordered (tetragonal structure) depending on oxygen content, temperature, and sample preparation. Numerous mixed  $\text{YBa}_2\text{Cu}_{3-x}\text{M}_x\text{O}_{7-y}$  ( $M=3d$  transition metal) phases have been synthesized and their structural, superconducting, and magnetic properties characterized.<sup>9-12</sup> Generally substitutions for Cu show a diminution of  $T_c$  as the doping concentration is increased. In order to investigate the relation of superconductivity and magnetic interactions, it is of interest to determine how the observed antiferromagnetic ordering in  $\text{YBa}_2\text{Cu}_3\text{O}_{7-y}$  is influenced by the substitution of a magnetic transition-metal atom for copper. Magnetic-susceptibility measurements on cobalt-substituted samples showed evidence that the antiferromagnetic coupling within  $\text{CuO}_2$  layers<sup>9</sup> is maintained in the substituted phase. Structural studies of these samples showed that Co

substitutes for Cu up to  $x=1$  and that it goes mainly into the  $\text{Cu}_{1-y}$  layers.<sup>9,12</sup> With increasing cobalt substitution  $T_c$  decreases continuously and is less than 4.2 K at  $x=0.4$ .<sup>10</sup>

In this work we present a neutron-powder-diffraction study on a sample of nominal composition  $\text{YBa}_2\text{Cu}_2\text{CoO}_7$ . Its crystal structure was refined and compared with the structure of other reported compounds of the series  $\text{YBa}_2\text{Cu}_{3-x}\text{Co}_x\text{O}_{7+y}$ . It is shown that the magnetic interactions give rise to 3D antiferromagnetic ordering and a model for the magnetic structure is derived from the observed superlattice peaks.

### EXPERIMENT

#### Sample preparation

Dried powders of  $\text{Y}_2\text{O}_3$ ,  $\text{BaCO}_3$ ,  $\text{CoCO}_3$ , and stoichiometric CuO were weighed out to produce a nominal composition  $\text{YBa}_2\text{Cu}_2\text{CoO}_{7+x}$ . These powders were ground together, pressed into a pellet, placed in a Pt crucible, heated in air to 1170 K, maintained at this temperature for one day, removed from the furnace at temperature, and cooled in air. The resulting material was reground, pelletized, and heated again in air at 1170 K for another day. After a final regrinding and pelletizing, the sample was heated in oxygen for two days at 1230 K, then for 4 h at 970 K, and finally furnace cooled to room temperature. Checks by x-ray powder diffraction showed the expected tetragonal phase together with a few small unidentified impurity peaks.

#### Oxygen content

The oxygen content was determined iodometrically by dissolving 0.1–0.2 g of finely ground sample and about 0.6

g of KI in 5 ml of HCl. To allow the powder to dissolve completely, the mixture was stirred, treated in an ultrasonic bath, and stirred again. The solution was added to 4–5-ml buffer solution (glacial acetic acid with  $\text{NH}_4\text{OH}$  added to give a  $\text{pH} \approx 3.5$ ) and titrated with standardized sodium thiosulfate. KSCN was added to desorb unreacted  $\text{I}_2$  in the later stages of the titration and starch was used as the end-point indicator.

#### Crystal structure

Neutron powder diffraction measurements were carried out on the triple-axis diffractometer H4S at the Brookhaven National Laboratory High Flux-Beam Reactor (HFBR). The experimental configuration consisted of a pyrolytic graphite monochromator and analyzer in the (002) and (004) settings, respectively, and the following collimation: 20' in-pile, 40' monochromator-sample, 40' sample-analyzer, and 20' analyzer-detector. The neutron wavelength was 2.3730(5) Å, a pyrolytic graphite filter being used to suppress higher-order wavelengths. The sample consisted of approximately 8 g of material in the form of a cylinder about 1 cm in diameter and 1.7 cm in height. The data were obtained at room temperature by step scanning at 0.1° intervals over a  $2\theta$  range of 8°–131°. The counting time for each data point was typically 30 sec.

#### Magnetic structure

Unpolarized neutron scattering measurements were performed on the triple-axis spectrometers H4S and H9A at the HFBR. Pyrolytic graphite crystals in the (002) setting were used for monochromator and analyzer. Most of the measurements were done with 5.0-meV neutrons ( $\lambda = 4.05$  Å), where a Be filter was used to eliminate higher-order contamination. The sample was mounted in an aluminum cylinder which was sealed inside an aluminum can filled with He exchange gas and then mounted on the cold finger of a Displex refrigerator. For measurements above room temperature, the sample cylinder was clamped in a furnace which was filled with a stagnant He atmosphere in order to avoid oxygen uptake at high temperatures. Some room-temperature measurements were also made with an incident energy of 14.7 meV ( $\lambda = 2.35$  Å) and pyrolytic graphite filters to extend the range of accessible wave vectors. The counting time for a data point was 3–15 min, depending on the expected intensity of the magnetic peak to be measured. Several peaks were measured a second time to increase the counting statistics.

### DATA ANALYSIS

#### Oxygen content

We assumed a valence of  $-2$  for oxygen and that Cu and Co reduce to  $\text{Cu}^{1+}$  and  $\text{Co}^{2+}$ , respectively. From the results of the titration an oxygen content corresponding to  $y = 0.23(3)$  can be calculated if we assume stoichiometric

$\text{YBa}_2\text{Cu}_2\text{CoO}_{7+y}$ . However, when we allow for the impurity phases and the actual metal-atom composition found by neutron powder diffraction, the corrected oxygen composition of the  $\text{YBa}_2\text{Cu}_{2.16}\text{Co}_{0.84}\text{O}_{7+y}$  phase is  $y = 0.31(4)$ .

#### Crystal structure

The structure refinement was carried out with a local version of the Rietveld-Hewat program.<sup>13,14</sup> The peaks, assumed to be Gaussian, with a small Lorentzian component to the peak profile, were described in the pseudo-Voigtian approximation and the background was refined together with the structure. The diffraction data were indexed on a tetragonal cell with no systematic absences (space group  $P4/mmm$ ,  $a = 3.8879$  Å,  $c = 11.636$  Å), similar to that of  $\text{YBa}_2\text{Cu}_3\text{O}_6$ . A few weak reflections, all smaller than 3% of the most intense reflection, could not be indexed with this cell and were excluded from the refinement. One of them was found to be a magnetic superlattice peak (see below), the others were presumed to be due to impurity phases. Two of the peaks were at positions corresponding to the (100) and (002) reflections of hexagonal Co. The  $\text{YBa}_2\text{Cu}_3\text{O}_6$  structure was used as a starting model, with Co on the Cu(1) site at (0,0,0) and an additional O(3) site at  $(\frac{1}{2}, 0, 0)$ . The occupancies of Co and Cu were allowed to vary independently on both the (0,0,0) and (0,0, $z$ ) sites. The total number of peaks in the refinement was 40. In the first refinements isotropic temperature factors were used and the occupancies of all oxygen sites were allowed to vary. At this stage the temperature factor for Co refined to a small negative value and the  $B$ 's of the transition metals were therefore restricted to be equal to reduce correlations between temperature factors and occupancies. Significant improvement was obtained with the introduction of an anisotropic temperature factor on the O(3) site or, alternatively, by using a statistical distribution of O(3) in a less symmetric site  $(\frac{1}{2}, y, 0)$ . The latter description was used in the final refinement. At the same time the occupancies of the two other oxygen sites, which had refined to 1.03(3) for O(1) and 0.97(2) for O(2), were set to one. The fit obtained with this model, using 27 parameters (scale factor, 14 atomic, 2 cell, 5 profile and 5 background parameters), is shown in Fig. 1 and the resulting structure model is given in Table I. The nearest-neighbor metal-oxygen distances calculated from this model are given in Table II. The cobalt content  $x = 0.84(4)$ , determined from neutron diffraction, is somewhat smaller than the nominal composition  $x = 1$ . We note, however, that the amount of the observed impurity phases may account for this discrepancy.

#### Magnetic structure

Diffraction peaks of magnetic origin were sought at 9 K by counting for much longer times at diffraction angles corresponding to superlattice indices of  $(1/2 \ 1/2 \ n/2)$ , for  $n = 0, 1, \dots, 7$  and for  $(\frac{1}{2} \ \frac{1}{2} \ \frac{1}{2})$ . Peaks at the expected positions were found at the latter position and at  $(1/2 \ 1/2 \ n/2)$  with  $n = 1, 3, 5$ . Scans of these peaks are

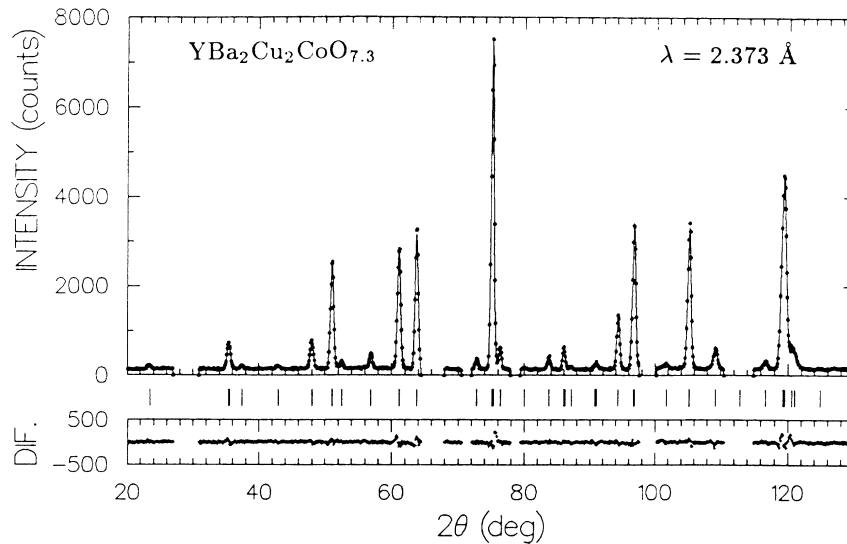


FIG. 1. Neutron-powder-diffraction data for  $\text{YBa}_2\text{Cu}_2\text{CoO}_{7.3}$  showing observed (dots), calculated (solid line), and difference plot (bottom). Short vertical markers represent allowed nuclear reflections.

shown in Fig. 2. The strongest one,  $(\frac{1}{2} \frac{1}{2} \frac{3}{2})$ , was in fact already observed in the 295-K data set used for the refinement of the nuclear structure. No evidence for peaks with  $n$  even was found. The upper intensity limit for peaks with  $n=0, 2$ , and  $6$  was 6% of the  $(\frac{1}{2} \frac{1}{2} \frac{3}{2})$  intensity. The existence of a small superlattice peak for  $n=4$  could not be ruled out due to an impurity peak close to this reflection.

Figure 3 illustrates the temperature dependence of the peak intensity measured for the  $(\frac{1}{2} \frac{1}{2} \frac{1}{2})$  and  $(\frac{1}{2} \frac{1}{2} \frac{3}{2})$  reflections up to a few degrees above the Néel temperature which was found to be at 405(3) K. The behavior was found to be reversible on cooling. Additional peaks

were measured at 147, 295, and 367 K, as listed in Table III. Integrated intensities were determined by fitting Gaussian-shaped profiles to the observed peaks. They are listed in Table III together with calculated values (see below) and the intensities of three nuclear peaks which were used for scaling.

All observed superlattice peaks could be indexed on a body-centered tetragonal magnetic unit cell with  $a_{\text{mag}} = a\sqrt{2}$ ,  $c_{\text{mag}} = 2c$ . This magnetic unit cell has four times the volume of the chemical one and consists of four  $\text{CuO}_2$  layers ( $A, A', C, C'$ ) and two Co-O layers (Ref. 20) ( $B, B'$ ) as can be seen in Fig. 4. For the following analysis we assume a collinear spin structure and that the magnetic mo-

TABLE I. Crystal structure of  $\text{YBa}_2\text{Cu}_{2.14}\text{Co}_{0.84}\text{O}_{7.32}$  at 295 K determined by Rietveld refinement. The numbers in parentheses are e.s.d.'s referred to the least significant digit. Scattering amplitudes for Ba, Y, Cu, Co, and O taken as 0.525, 0.775, 0.7717, 0.253, and  $0.5805 \times 10^{-12}$  cm, respectively (Ref. 15). Space group:  $P4/mmm$ . Atomic parameters.

		$x$	$y$	$z$	$B$ ( $\text{\AA}^2$ )	$N^a$
Y	in $1d$	$\frac{1}{2}$	$\frac{1}{2}$	$\frac{1}{2}$	0.4(2)	1.0
Ba	in $2h$	$\frac{1}{2}$	$\frac{1}{2}$	0.1870(4)	0.0(2)	2.0
Cu(1)	in $1a$	0	0	0	0.8(2) <sup>b</sup>	0.20(2) <sup>b</sup>
Co(1)	in $1a$	0	0	0	0.8(2) <sup>b</sup>	0.80(2) <sup>b</sup>
Cu(2)	in $2g$	0	0	0.3595(3) <sup>b</sup>	0.8(2) <sup>b</sup>	1.96(4) <sup>b</sup>
Co(2)	in $2g$	0	0	0.3595(3) <sup>b</sup>	0.8(2) <sup>b</sup>	0.04(4) <sup>b</sup>
O(1)	in $2g$	0	0	0.1568(5)	1.4(2)	2.0
O(2)	in $4i$	0	$\frac{1}{2}$	0.3772(3)	0.1(2)	4.0
O(3)	in $4n$	0.081(4)	$\frac{1}{2}$	0	0.2(2)	1.32(4)

Unit cell<sup>c</sup> ( $\text{\AA}$ ):  $a = 3.8879(8)$ ,  $c = 11.636(3)$   
 Agreement factors<sup>d</sup>:  $R_I = 0.055$ ,  $R_{wp} = 0.078$ ,  $S_p^2 = 2.3$ ,  $S_f^2 = 3.8$

<sup>a</sup>Number of atoms per formula unit.

<sup>b</sup>Constraint parameters:  $B_{\text{Cu}(1)} = B_{\text{Co}(1)} = B_{\text{Cu}(2)} = B_{\text{Co}(2)}$ ,  $N_{\text{Cu}(1)} + N_{\text{Co}(1)} = 1.0$ ,  $N_{\text{Cu}(2)} + N_{\text{Co}(2)} = 2.0$ ,  $z_{\text{Cu}(2)} = z_{\text{Co}(2)}$ .

<sup>c</sup>e.s.d.'s include uncertainties on neutron wavelength [ $\lambda = 2.3730(5)$   $\text{\AA}$ ].

<sup>d</sup>For definitions see Ref. 16.

TABLE II. Oxygen-metal bond distances.

YBa <sub>2</sub> Cu <sub>2.16</sub> Co <sub>0.84</sub> O <sub>7.32</sub> (this work)			YBa <sub>2</sub> Cu <sub>3</sub> O <sub>7</sub> (Ref. 17)		
	Distance (Å)	<i>n</i> <sup>a</sup>		Distance (Å)	<i>n</i> <sup>a</sup>
Co(1)-O(1) <sup>b</sup>	1.824(5)	2	Cu(1)-O(1) <sup>b</sup>	1.853(3)	2
Co(1)-O(3)	1.969(3)	2.64	Cu(1)-O(4)	1.941	2
Cu(2)-O(1)	2.359(6)	1	Cu(2)-O(1)	2.285(4)	1
Cu(2)-O(2)	1.955(1)	4	{ Cu(2)-O(2)	1.928(1)	2
			{ Cu(2)-O(3)	1.960(1)	2
Ba-O(1)	2.772(1)	4	Ba-O(1)	2.738(1)	4
Ba-O(2)	2.946(3)	4	{ Ba-O(2)	2.986(4)	2
			{ Ba-O(3)	2.962(4)	2
Ba-O(3)	2.718(9)	1.32	{ Ba-O(4)	2.871(3)	2
Ba-O(3)	3.136(9)	1.32			
Y-O(2)	2.413(3)	8	{ Y-O(2)	2.406(2)	4
			{ Y-O(3)	2.382(2)	4

<sup>a</sup>*n* is the average number of equivalent bonds.

<sup>b</sup>The numbering of the oxygen atoms is different in the two structures due to different structural symmetries. Corresponding bond lengths are listed on the same line.

ments are localized at the Cu and Co sites. The fact that *h*, *k*, and *l* are odd has two implications: first, nearest-neighbor Cu (or Co) atoms within a layer have antiparallel magnetic moments, just as observed in YBa<sub>2</sub>Cu<sub>3</sub>O<sub>7-*y*</sub> (Ref. 5) and La<sub>2</sub>CuO<sub>4-*y*</sub> (Ref. 4), and second, two atoms separated by *c*, i.e., belonging to either *A* and *A'*, *B* and *B'*, or *C* and *C'*, respectively, have antiparallel spins as well. The remaining problem is then to determine the stacking phase of the magnetic moments in the three layers *A*, *B*, and *C* along the *c* axis.

The magnetic structure factor for collinear spin structure, normalized to the chemical unit cell, is

$$F_{hkl}^M = i \sin(\pi h) \sin(\pi k) \sin(\pi l) (p_A e^{i2\pi z l} + p_B + p_C e^{-i2\pi z l}),$$

where *p<sub>A</sub>*, *p<sub>B</sub>*, *p<sub>C</sub>* are the amplitude factors for the *A*, *B*, and *C* antiferromagnetic layers and *z* is the fraction of a

unit-cell length *c* by which the *A* and *C* layers are displaced from *B*. Each amplitude factor *p<sub>i</sub>* is given by

$$p_i = \pm \gamma_0 M_i f(Q) \sin \eta,$$

where  $\gamma_0 = (0.269 \times 10^{-12} \text{ cm}) / \mu_B$ , *M<sub>i</sub>* is the average ordered magnetic moment (in Bohr magnetons  $\mu_B$ ) in the *i*th layer, *f(Q)* is the magnetic form factor for the Cu or Co atoms, and  $\eta$  is the angle between the scattering vector *Q* and the direction of the magnetic moment.

Let us first assume, by analogy to YBa<sub>2</sub>Cu<sub>3</sub>O<sub>6+*y*</sub>, that only the layers *A* and *C* have a magnetic moment. From the symmetry of the lattice, we assume that *M<sub>A</sub>* = *M<sub>C</sub>*, and thus we are left with the two choices (a) *p<sub>A</sub>* = *p<sub>C</sub>* or (b) *p<sub>A</sub>* = -*p<sub>C</sub>*. A further unknown is the spin direction. As the symmetry of the lattice is tetragonal, the most that can be determined from powder-diffraction measurements

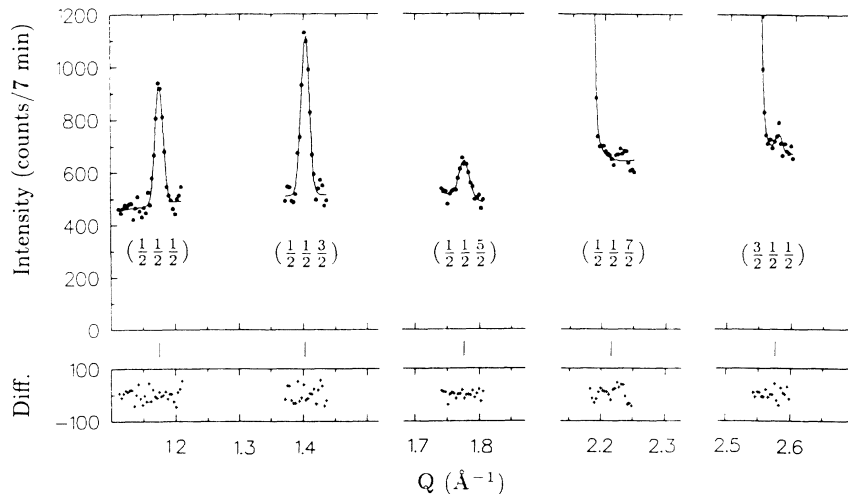


FIG. 2. Neutron diffraction scans of several magnetic peaks for YBa<sub>2</sub>Cu<sub>2</sub>O<sub>7.3</sub> measured at 9 K. The lines are least-squares fits assuming Gaussian peak profiles.

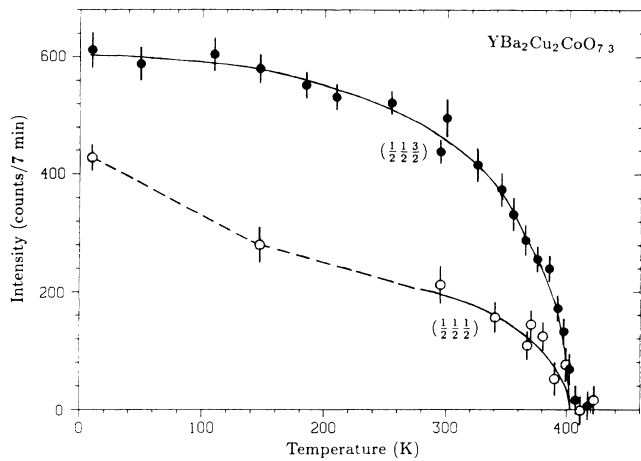


FIG. 3. Difference between peak and background intensities for the  $(\frac{1}{2} \frac{1}{2} \frac{1}{2})$  (open circles) and  $(\frac{1}{2} \frac{1}{2} \frac{3}{2})$  (filled circles) magnetic reflections in  $\text{YBa}_2\text{Cu}_2\text{CoO}_{7.3}$  as a function of temperature. The intensities have been normalized at 295 K to allow for the different experimental conditions under which the data were collected above and below room temperature. Solid and dashed lines are drawn as a guide to the eye.

is the angle between the magnetic moment and the  $c$  axis. It is most likely that the spins either lie in the plane or are perpendicular to it, and hence we limited our analysis to these two choices. Intensities were calculated and fitted to the observed intensities for the two spin directions and the two models (a) and (b), refining  $M_A$  as a parameter. No agreement could be obtained for case (a) for either spin direction. Good agreement was obtained for case (b) at 295 and 367 K, with  $M_A = [0.65(5)]\mu_B$  and  $M_C = [0.54(5)]\mu_B$ , respectively, and spins along the  $c$  axis. However, at 9 K, the agreement was much less satisfactory. This is most clearly seen from the ratio of  $I(\frac{1}{2} \frac{1}{2} \frac{1}{2}) : I(\frac{1}{2} \frac{1}{2} \frac{3}{2})$  which is calculated to be 0.42 whereas the observed value is much greater, namely, 0.78(5). A similar, but less pronounced trend is seen at 147 K where the ratio is 0.57(4). To attempt to account for these discrepancies, we allow a small magnetic moment  $\mu_B$  in the Co layer either parallel or antiparallel to the two Cu atoms above and below them and refined now the two parameters  $M_A$  and  $M_B$ . The obtained fit for the 9 and 147 K was satisfactory for all spins along the  $c$  axis and yielded the following average magnetic moments:  $M_A = [0.87(7)]\mu_B$ ,  $M_B = [0.16(2)]\mu_B$  at 9 K, and

TABLE III. Comparison of integrated intensities of magnetic reflections observed (scaled intensities; e.s.d.'s are given in parentheses and refer to the least significant digit) ( $I_{\text{obs}}$ ) and calculated [Freeman-Watson form factors in the spherical approximation for  $\text{Cu}^{2+}$  (Ref. 18) and  $\text{Co}^{3+}$  (Ref. 19) were used for moments on Cu and Co, respectively] ( $I_{\text{calc}}$ ) for  $\text{YBa}_2\text{Cu}_{2.14}\text{Co}_{0.84}\text{O}_{7.32}$  for model shown in Fig. 4.

$(hkl)$	$Q$ ( $\text{\AA}^{-1}$ ) <sup>a</sup>		9 K	147 K	295 K	367 K
$(\frac{1}{2} \frac{1}{2} \frac{1}{2})$	1.174	$I_{\text{obs}}$	118(4)	85(5)	43(3)	29(6)
		$I_{\text{calc}}$	112	79	39	29
$(\frac{1}{2} \frac{1}{2} \frac{3}{2})$	1.401	$I_{\text{obs}}$	152(9)	149(5)	105(3)	70(6)
		$I_{\text{calc}}$	147	147	104	69
$(\frac{1}{2} \frac{1}{2} \frac{5}{2})$	1.769	$I_{\text{obs}}$	40(4)	32(4)	16(3)	16(5)
		$I_{\text{calc}}$	51	42	23	17
$(\frac{1}{2} \frac{1}{2} \frac{7}{2})$	2.209	$I_{\text{obs}}$	3(4)	12(9)	3(4)	
		$I_{\text{calc}}$	0	0	0	
$(\frac{3}{2} \frac{1}{2} \frac{1}{2})$	2.569	$I_{\text{obs}}$	26(6)		8(3)	
		$I_{\text{calc}}$	30		11	
$(\frac{3}{2} \frac{1}{2} \frac{3}{2})$	2.890	$I_{\text{obs}}$			18(9)	
		$I_{\text{calc}}$			22	
$(\frac{3}{2} \frac{3}{2} \frac{1}{2})$	3.439	$I_{\text{obs}}$			-1(4)	
		$I_{\text{calc}}$			2	
Ordered magnetic moments (in $\mu_B$ )						
On Cu			0.87(7)	0.82(6)	0.65(5)	0.54(5)
On Co			0.16(2)	0.06(2)	0.02(2)	0.00(4)
Nuclear peaks used as reference						
(001)	0.540	$I_{\text{obs}}$	4550(90)	4810(90)	5140(95)	
		$I_{\text{calc}}$			4835 <sup>b</sup>	
(100)/(003)	$\approx 1.618$	$I_{\text{obs}}$	1465(40)	1445(50)	1335(30)	
		$I_{\text{calc}}$			1425 <sup>b</sup>	
(004)	2.160	$I_{\text{obs}}$	1305(70)	1425(60)	1405(30)	
		$I_{\text{calc}}$			1400 <sup>b</sup>	

<sup>a</sup> $Q$  is the absolute value of the wave vector, given for the 295-K data.

<sup>b</sup>Calculated intensities from Rietveld structure refinement.

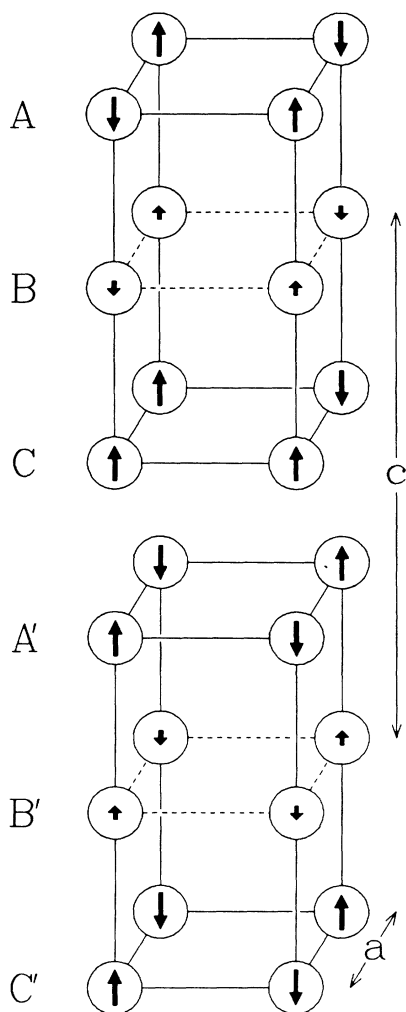


FIG. 4. Proposed low-temperature magnetic structure for  $\text{YBa}_2\text{Cu}_2\text{CoO}_{7.3}$ . The circles represent the Cu and Co atoms and the arrows their respective moments at 9 K. The arrows point in the direction of the average order moments. Solid lines connect pairs of transition-metal sites bridged by oxygen atoms, dashed lines indicate possible bridges via partially occupied oxygen sites. Two full chemical units cells are shown stacked vertically; the magnetic unit cell has the height of two chemical cells and double the area in the basal plane.

$M_A = [0.82(6)]\mu_B$ ,  $M_B = [0.06(2)]\mu_B$  at 147 K. A comparison of calculated and observed integrated intensities is given in Table III, and the resulting magnetic structure is shown in Fig. 4. It should be mentioned that a model using small in-plane moments in the  $B$  layer and moments parallel to  $c$  in layers  $A$  and  $C$  can explain the data almost as well, but this seems unlikely, because the fourfold symmetry of the magnetic structure is lost and the moments in the  $B$  layer would be decoupled from those in layers  $A$  and  $C$ .

#### DISCUSSION

The perovskite-type structure of  $\text{YBa}_2\text{Cu}_3\text{O}_7$  has two distinct copper sites, one with a square-planar oxygen

configuration [Cu(1)] forming O-Cu-O chains and the other with square-pyramidal configuration [Cu(2)], forming sheets of  $\text{CuO}_2$ .<sup>8</sup> It was shown<sup>9-11</sup> that, upon substitution, Co preferentially replaces Cu in the Cu(1) sites. The structure refinement of the present sample showed no significant amounts of Co in the Cu(2) site, in contrast to a previous neutron-powder-diffraction study<sup>10</sup> on a  $\text{YBa}_2\text{Cu}_{3-x}\text{Co}_x\text{O}_{7+y}$  sample ( $x = 0.8$ ) for which 12% of the Co was found on the Cu(2) site. The total oxygen content of 7.32 derived from the neutron-powder-diffraction data agrees well with the chemical oxygen analysis and with those found in other oxygen-annealed samples.<sup>9,10</sup> The unit cell of the present sample ( $a = 3.888$  Å,  $c = 11.363$  Å) is comparable with those reported<sup>9,10</sup> for  $\text{YBa}_2\text{Cu}_{3-x}\text{Co}_x\text{O}_{7+y}$  samples with  $x = 0.8-1.0$  but significantly different from values reported for samples with  $x \leq 0.5$ .<sup>10,11</sup> Whereas the length of the  $a$  axis depends mainly on the amount of substituted cobalt, the length of the  $c$  axis is also dependent on the oxygen content. The general trend of an increasing  $c$  axis with decreased oxygen content found for the unsubstituted  $\text{YBa}_2\text{Cu}_3\text{O}_{7-y}$  series seems to apply also for the cobalt-substituted samples. Thus the relatively short axis of the present sample together with its rather high oxygen content is in good agreement with this trend. The refined atomic positional parameters (see Table I) are in good agreement with those obtained in a single-crystal x-ray diffraction study<sup>9</sup> on a  $\text{YBa}_2\text{Cu}_2\text{CoO}_{7.25}$  sample.

Let us now compare the structure of the cobalt-substituted compound with that of the  $\text{YBa}_2\text{Cu}_3\text{O}_{7-x}$  series. For the latter series the most evident changes in the local structure of the  $\text{CuO}_2$  layer upon removal of oxygen are the shifts of O(1) away from Cu(2) and of Ba towards the  $\text{CuO}_2$  layer. The Cu(2)-O(1) distance (2.36 Å) as well as the displacement of Ba from the plane containing O(2) (2.21 Å) found in the cobalt-substituted sample corresponds to those in  $\text{YBa}_2\text{Cu}_3\text{O}_{7-x}$  with an intermediate oxygen content ( $x \approx 0.5$ ).<sup>21</sup> Therefore we may assume that the electron distribution in the  $\text{CuO}_2$  layer is basically the same as in  $\text{YBa}_2\text{Cu}_3\text{O}_{6.5}$ , for which the average copper valence is +2. Considering the oxygen content of the  $\text{YBa}_2\text{Cu}_{2.14}\text{Co}_{0.84}\text{O}_{7.32}$  sample we may conclude that the oxidation state of the substituting Co exceeds that of Cu(1) by 1, which is consistent with the assumption of the trivalent cobalt.

The main changes of the local structure are expected in the layer where the substitution takes place. Due to its higher oxidation state, cobalt tends to have a higher coordination number. Chemical analysis of the oxygen content and the structure refinement of the neutron-diffraction data have confirmed this point. We might expect the cobalt atom to be five coordinated, probably in square-pyramidal coordination, which is not unusual for trivalent cobalt, e.g., in  $\text{Sr}_2\text{Co}_2\text{O}_5$ .<sup>22</sup> This nonplanar coordination breaks up the long-range oxygen order induced by the O-Cu-O chains present in orthorhombic  $\text{YBa}_2\text{Cu}_3\text{O}_{7-y}$ , thus favoring tetragonal symmetry for the Co-substituted samples. The displacement of the O(3) from the site  $(0, \frac{1}{2}, 0)$  and the apparent increased temperature factor of O(1) found in our structure refinement as well as in the single-crystal x-ray diffraction study,<sup>9</sup> may be a

consequence of local displacements due to the formation of square  $\text{CoO}_5$  pyramids whose basal O-Co-O angles for adjacent oxygens are likely to be smaller than  $180^\circ$ .

In  $\text{YBa}_2\text{Cu}_{2.14}\text{Co}_{0.84}\text{O}_{7.32}$  the Cu moments have the same local antiferromagnetic ordering within the  $\text{CuO}_2$  layer as in  $\text{La}_2\text{CuO}_4$  (Ref. 4) and  $\text{YBa}_2\text{Cu}_3\text{O}_{6+x}$ .<sup>5</sup> Superexchange interactions via the oxygen bridges are responsible for this in-plane ordering. Another structural feature shared with the latter compound is the antiparallel arrangement of two adjacent Cu moments in neighboring *A* and *C* layers. Since these copper atoms are not bridged by oxygen, the magnetic interaction should be mostly dipolar. The magnetic structure of the cobalt-substituted sample differs, however, from that reported for  $\text{YBa}_2\text{Cu}_3\text{O}_{6+x}$  in the following respects. Not only is the direction of the moments found to be parallel to *c*, but the long-range order has double the periodicity along the *c* axis. However, in a recent study of  $\text{YBa}_2\text{Cu}_3\text{O}_{6+x}$  single crystal with  $x \approx 0.35$  and  $T_N = 405$  K, Kadowaki *et al.*<sup>23</sup> have observed  $(1/2, 1/2, n/2)$  peaks below 40 K, indicating long-range magnetic order with a double *c* axis. This experiment also demonstrated that the *B* layers can contribute to the magnetic ordering. The same type of magnetic ordering was found recently in  $\text{NdBa}_2\text{Cu}_3\text{O}_{6.1}$ .<sup>24</sup> As for the cobalt-substituted sample, the small ordered moments in the *B* layer are parallel to the adjacent moments in the neighboring  $\text{CuO}_2$  layers.

The ordered moment of  $0.87\mu_B$  observed at 9 K on Cu(2) is considerably higher than the moments of  $0.68\mu_B$  found in CuO (Ref. 25) and the maximum values obtained in  $\text{La}_2\text{CuO}_{4-y}$  (Ref. 4) and  $\text{YBa}_2\text{Cu}_3\text{O}_{6+x}$ .<sup>5</sup> Assuming a *g* factor of  $\sim 2.2$ , typical for  $\text{Cu}^{2+}$  ions, and a classical spin of  $\frac{1}{2}$ , a maximum moment of  $1.1\mu_B$  might be expected. The observed value may be lower due to quantum fluctuation and/or covalency effects. Considering quantum fluctuations in a completely isotropic 2D Heisenberg system, the moment would be reduced to  $0.67\mu_B$ . The observed value is greater than this which is an indication that the interlayer coupling induced by the magnetic moments in the Co layers is not negligible.

The Néel temperature of 405 K found in our sample is comparable to those found for  $\text{YBa}_2\text{Cu}_3\text{O}_{6+x}$ , with  $x < 0.3$ . In layered systems the Néel temperature is generally assumed to be proportional to an effective interplanar coupling  $J_{\perp}^{\text{eff}}$  and the square of a magnetic correlation length  $\xi_{2D}$  within a layer. Therefore stronger interplanar coupling should raise the Néel temperature. On the other hand,  $\xi_{2D}$  may well be shorter in the cobalt-substituted sample. As pointed out earlier, the electronic structure of its  $\text{CuO}_2$  layers is comparable to that of  $\text{YBa}_2\text{Cu}_3\text{O}_{6.5}$ . At this oxygen composition the proposed formation of electron holes, localized on the O atoms,<sup>26</sup> may play a role. These holes tend to frustrate the Cu-Cu superexchange in-

teractions<sup>2,27</sup> thus shortening the magnetic correlation length.

We may assume that the interaction between adjacent Cu moments in next-nearest *A* and *C* layers is induced mainly by the Co moments between them. Then, symmetry arguments require that the two Cu atoms have parallel moments, independent of the nature of the Cu-Co interaction. This explains the long-range order in the *c* direction with a period of  $2c$ . Interestingly, this long-range order is maintained up to the Néel temperature of 405 K, even though the ordered magnetic moment on the Co layer vanishes well below this temperature. The question arises as to the nature of the magnetic moments in the Co layer. The small but significant ordered magnetic moment per metal atom at 9 K ( $0.16\mu_B$ ) could conceivably be explained if there were about  $0.8\mu_B$  on the remaining one-fifth of Cu atoms and the (0,0,0) sites, assuming no ordered moment on Co. This seems rather unlikely considering the magnetic structure of unsubstituted samples. The assumption of a small but finite ordered moment on the Co atoms has implications concerning its possible spin state. For low-spin Co(III) no magnetic moment would be expected. On the other hand, much higher moments are typically found for high spin  $\text{Co}^{3+}$ . So we may consider an intermediate spin state, close to Co(III). Intermediate spin states of trivalent cobalt have also been found in other oxides<sup>22,28</sup> and have been considered<sup>10</sup> in order to explain magnetic susceptibility measurements on other samples of the  $\text{YBa}_2\text{Cu}_{3-x}\text{Co}_x\text{O}_{7+y}$  series. However, the magnetic moments attributed to the cobalt atom [ $(3-4)\mu_B$ ] to explain the latter data are much higher than our data would suggest. To be consistent, we would have to assume that the direction of the Co moments are highly disordered, leaving only a small average moment parallel to the adjacent Cu atoms above and below them, which upon heating disappears before the Néel temperature is reached. This kind of disorder might be induced by competing ferromagnetic and antiferromagnetic interactions within the Co layers.

#### ACKNOWLEDGMENTS

We are grateful to A. R. Moodenbaugh for his assistance in sample preparation and to J. Michel for double checking the oxygen analysis at E. I. du Pont de Nemours, Wilmington, DE. This work was supported by the U.S. Department of Energy (Division of Materials Sciences, Office of Basic Energy Sciences) under Contract No. DE-AC02-76CH00016. One of us (P.Z.) gratefully acknowledges financial support from the Swiss National Science Foundation.

<sup>1</sup>See, for example, J. G. Bednorz and K. A. Müller, *Z. Phys. B* **64**, 189 (1986); M. K. Wu, J. R. Ashburn, C. J. Torng, P. H. Hor, R. L. Meng, L. Gao, Z. J. Huang, Y. Q. Wang, and C. W. Chu, *Phys. Rev. Lett.* **58**, 908 (1987); M. Maeda, Y. Tanaka, M. Fukutomi, T. Asano, *Jpn. J. Appl. Phys.* **97**, Pt. 2, L209 (1988).

<sup>2</sup>V. J. Emery, *Phys. Rev. Lett.* **58**, 2794 (1987).

<sup>3</sup>P. W. Anderson, *Science* **235**, 1196 (1987); J. E. Hirsch, *Phys. Rev. Lett.* **59**, 228 (1987); S. A. Kivelson, D. S. Rokhsar, and J. P. Sethna, *Phys. Rev. B* **35**, 8865 (1987); A. E. Ruckenstein, P. J. Hirschfeld, and J. Appel, *ibid.* **36**, 857 (1987); M. Cyrot, *Solid State Commun.* **62**, 821 (1987).

- <sup>4</sup>R. L. Greene, H. Maletta, T. S. Plaskett, J. G. Bednorz, and K. A. Müller, *Solid State Commun.* **63**, 379 (1987); D. Vaknin, S. K. Sinha, D. E. Moncton, D. C. Johnston, J. M. Newsam, C. R. Safinya, and H. E. King, Jr., *Phys. Rev. Lett.* **58**, 2802 (1987); Y. Yamaguchi, H. Yamauchi, M. Ohashi, H. Yamamoto, N. Shimoda, M. Kikuchi, and Y. Syono, *Jpn. J. Appl. Phys.* **26**, Pt. 2, L447 (1987); S. Mitsuda, G. Shirane, S. K. Sinha, D. C. Johnston, M. S. Alvarez, D. Vaknin, and D. E. Moncton, *Phys. Rev. B* **36**, 822 (1987); T. Freltoft, J. E. Fischer, G. Shirane, D. E. Moncton, S. K. Sinha, D. Vaknin, J. P. Remeika, A. S. Cooper, and D. Harshman, *ibid.* **36**, 826 (1987); D. C. Johnston, J. P. Stokes, D. P. Goshorn, and J. T. Lewandowski, *ibid.* **36**, 4007 (1987).
- <sup>5</sup>J. M. Tranquada, D. E. Cox, W. Kunnmann, H. Moudden, G. Shirane, M. Suenaga, P. Zolliker, D. Vaknin, S. K. Shina, M. S. Alvarez, A. J. Jacobson, and D. C. Johnston, *Phys. Rev. Lett.* **60**, 156 (1988); J. M. Tranquada, A. H. Moudden, A. I. Goldman, P. Zolliker, D. E. Cox, G. Shirane, S. K. Sinha, D. Vaknin, D. C. Johnston, M. S. Alvarez, A. J. Jacobson, J. T. Lewandowski, and J. M. Newsam, *Phys. Rev. B* **38**, 2477 (1988).
- <sup>6</sup>W.-H. Li, J. W. Lynn, H. A. Mook, B. C. Sales, and Z. Fisk, *Phys. Rev. B* **37**, 9844 (1988); J. Rossat-Mignod, P. Burlet, M. J. G. M. Jurgens, J. Y. Henry, and C. Vettier (unpublished).
- <sup>7</sup>G. Shirane, Y. Endoh, R. J. Birgenau, M. A. Kastner, Y. Hidaka, M. Oda, M. Suzuki, and T. Murakami, *Phys. Rev. Lett.* **59**, 1613 (1987); Y. Endoh, K. Yamada, R. J. Birgenau, D. R. Gabbe, H. P. Janssen, M. A. Kastner, C. J. Peters, P. J. Picone, T. R. Thurston, J. M. Tranquada, G. Shirane, Y. Hidaka, M. Oda, Y. Enomoto, M. Suzuki, and T. Murakami, *Phys. Rev. B* **37**, 7443 (1988); C. J. Peters, R. J. Birgenau, M. A. Kastner, H. Yoshizawa, Y. Endoh, J. M. Tranquada, G. Shirane, Y. Hidaka, M. Oda, M. Suzuki, and T. Murakami, *ibid.* **37**, 9761 (1988).
- <sup>8</sup>For a review, see J. D. Jorgensen, *Jpn. J. Appl. Phys.* **26**, 2017 (1987).
- <sup>9</sup>Y. K. Tao, J. S. Swinnea, A. Manthiram, J. S. Kim, J. B. Goodenough, and H. Steinfink, *J. Mater. Res.* **3**, 248 (1988).
- <sup>10</sup>J. M. Tarascon, P. Barboux, P. F. Miceli, L. H. Greene, G. W. Hull, M. Eibschutz, and S. A. Sunshine, *Phys. Rev. B* **37**, 7458 (1988); P. F. Miceli, J. M. Tarascon, L. H. Greene, P. Barboux, F. J. Rotella, and J. D. Jorgensen, *ibid.* **37**, 5932 (1988).
- <sup>11</sup>T. Kajitani, K. Kusaba, M. Kikuchi, Y. Syono, and M. Hirabayashi, *Jpn. J. Appl. Phys.* **26**, L1727 (1987).
- <sup>12</sup>Y. Maeno, T. Tomita, M. Kyogoku, S. Awaji, Y. A. Oki, K. Hoshino, A. A. Minami, and T. Fujita, *Nature* **328**, 512 (1987); G. Xiao, F. H. Streitz, A. Gavrin, Y. W. Du, and C. L. Chien, *Phys. Rev. B* **35**, 8782 (1987).
- <sup>13</sup>H. M. Rietveld, *J. Appl. Crystallogr.* **2**, 65 (1969).
- <sup>14</sup>A. W. Hewat, United Kingdom Atomic Energy Research Establishment, Harwell, Report No. R7350, 1973 (unpublished).
- <sup>15</sup>L. Koester and H. Rauch, International Atomic Energy Agency Report No. 2517/RB, 1981 (unpublished).
- <sup>16</sup>H. G. Scott, *J. Appl. Crystallogr.* **16**, 159 (1983).
- <sup>17</sup>D. E. Cox, A. R. Moodenbaugh, J. J. Hurst, and R. H. Jones, *J. Phys. Chem. Solids* **48**, 42 (1987).
- <sup>18</sup>T. Freltoft, G. Shirane, S. Mitsuda, J. P. Remieka, and A. S. Cooper, *Phys. Rev. B* **37**, 137 (1988).
- <sup>19</sup>R. E. Watson and A. J. Freeman, *Acta Crystallogr.* **14**, 27 (1961).
- <sup>20</sup>For simplicity we use here and later on the term "Co layer," even if this layer also contains small amounts of unsubstituted Cu.
- <sup>21</sup>S. Miraglia, F. Beech, A. Santoro, and D. Tran Qui, *Mater. Res. Bull.* **22**, 1733 (1987); D. C. Johnston, A. J. Jacobson, J. M. Newsam, J. T. Lewandowski, and D. P. Goshorn, in *Chemistry of High-Temperature Superconductors*, edited by D. L. Nelson, M. S. Whittingham, and T. F. George, ACS Symposium Series, Vol. 351 (American Chemical Society, Washington, DC, 1987), pp. 136–151.
- <sup>22</sup>J.-C. Grenier, S. Ghodbane, G. Demazeau, M. Pouchard, and P. Hagenmuller, *Mater. Res. Bull.* **14**, 831 (1979).
- <sup>23</sup>H. Kadowaki, M. Nishi, Y. Yamada, H. Takeya, H. Takei, S. M. Shapiro, and G. Shirane *Phys. Rev. B* **37**, 7932 (1988).
- <sup>24</sup>A. H. Moudden, G. Shirane, J. M. Tranquada, R. J. Birgenau, Y. Endoh, K. Yamada, Y. Hidaka, and T. Murakami, *Phys. Rev. B* (to be published).
- <sup>25</sup>B. N. Brockhouse, *Phys. Rev.* **94**, A781 (1954); B. X. Yang, J. M. Tranquada, and G. Shirane, *Phys. Rev. B* **38**, 174 (1988).
- <sup>26</sup>J. M. Tranquada, S. M. Heald, and A. R. Moodenbaugh, *Phys. Rev. B* **36**, 5263 (1987); N. Nücker, J. Fink, J. C. Fuggle, P. J. Durham, and W. M. Temmerman, *ibid.* **37**, 5158 (1988); Z. Shen, J. W. Allen, J. J. Yeh, J.-S. Kang, W. Ellis, W. Spicer, I. Landau, M. B. Maple, Y. D. Dalichaouch, M. S. Torikachvili, and J. Z. Sun, *ibid.* **36**, 8414 (1987).
- <sup>27</sup>A. Aharoni, R. J. Birgenau, A. Coniglio, M. A. Kastner, and H. E. Stanley, *Phys. Rev. Lett.* **60**, 1330 (1988).
- <sup>28</sup>G. Thornton, B. C. Tofield, and A. W. Hewat, *J. Solid State Chem.* **61**, 301 (1986).